1 Review of semiconductor materials and physics

1.1 Executive summary

Semiconductor devices are fabricated using specific materials that offer the desired physical properties. There are three classes of solid state materials: insulators, semiconductors and conductors. This distinction is based on the electrical conductivity of these materials with insulators having the lowest and conductors having the highest conductivity. Semiconductors fall in between and their conductivity is affected by several factors such as temperature, the incidence of light, the application of a magnetic field and impurities. This versatility makes semiconductors very important in electronics and optoelectronics applications.

Semiconductors themselves are divided into two classes: elemental and compound. Each type has distinctive physical properties which are exploited in device design. Typical elemental semiconductor device materials are silicon and germanium; examples of compound semiconductors are GaAs, InP, AlGaAs and SiGe. The single crystal structure of these materials is that of a periodic lattice and this determines the properties of the semiconductors. Silicon has the diamond crystal structure and the compound semiconductors have the zincblende lattice structure. The bonding between atoms in a crystal of the semiconductors is termed *covalent bonding*, where electrons are shared between atoms. Fundamental principles of quantum mechanics are applied to determine the energy band structure of the semiconductor.

The basic device physics involves the description of the energy band structure, the density of states, the carrier concentration and the definition of donors and acceptors. Semiconductors are categorised as direct or indirect depending on the bandgap. The absorption mechanism is described and radiation and recombination processes important to device performance are detailed. The two carrier transport processes are drift and diffusion. The currents due to these transport processes are expressed in terms of the applied electric field, the carrier mobility and the carrier concentration. The junction formed by p-type semiconductor (excess holes) and n-type semiconductor (excess electrons) is described and the characteristics of such a junction are given. The important Schottky diode, a junction formed by a metal and a semiconductor layer (n-doped in this case) is characterised.

Heterostructures formed by dissimilar semiconductors are important in device design. The properties of heterojunctions of semiconductor materials are presented. Silicon–germanium heterojunctions are of particular interest as high performance electronic

Table 1.1 Portion of the periodic table showing semiconductor material elements

Period	Group III	Group IV	Group V
2	B Boron	C Carbon	N Nitrogen
3	Al Aluminium	Si Silicon	P Phosphorus
4	Ga Gallium	Ge Germanium	As Arsenic
5	In Indium	Sn Tin	Sb Antimony

Table 1.2 Elemental and binary compound semiconductors

Elements	IV–IV Binary compounds	III–V Binary compounds
Si Silicon Ge Germanium	SiC Silicon carbide SiGe Silicon germanium	AlAs Aluminium arsenide AlP Aluminium phosphide AlSb Aluminium antimonide BN Boron nitride GaAs Gallium arsenide GaN Gallium nitride GaSb Gallium antimonide InAs Indium arsenide InP Indium phosphide InSb Indium antimonide

Table 1.3 Ternary and quaternary semiconductors

Ternary compounds	Quaternary compounds
$Al_xGa_{1-x}As$ Aluminium gallium arsenide	$Al_xGa_{1-x}As_ySb_{1-y}$ Aluminium gallium arsenic antimonide
$GaAs_{1-x}P_x$ Gallium arsenic phosphide	$Ga_xIn_{1-x}As_{1-y}P_y$ Gallium indium arsenic phosphide

devices have been designed using this material alloy. This chapter gives a detailed discussion of these heterojunctions.

1.2 Semiconductor materials

Materials used for semiconductors fall into two categories: elemental semiconductors and compound semiconductors. Table 1.1 shows the section in the periodic table which has the semiconductor elements and Table 1.2 lists examples for elemental and binary compound semiconductors. Some ternary and quaternary semiconductors are listed in Table 1.3.

1.3 Types of solids

There are three types of solids: crystalline, polycrystalline and amorphous. The arrangement of atoms is periodic in three dimensions in a crystalline solid with forces binding the atoms together. This periodicity exists over the entire crystal and it will appear the same regardless of the region where the crystal is viewed. If the periodicity of the atoms occurs over a small region of the solid and changes in different regions of the solid, the solid is termed to be *polycrystalline*. Atoms in amorphous solids exhibit no periodicity. Figure 1.1 shows the three different types of solids.

1.4 Crystal structure

Semiconductor materials such as Si, Ge and GaAs that are to be used for devices are crystalline, that is, a single crystal. This periodic arrangement of atoms in a crystal is termed a *lattice* and the distance between the atoms is the *lattice constant*. The unit cell is a fundamental unit in the crystal and a repetition of the unit cell generates the entire lattice. The unit cell is not unique and can be chosen in various ways as shown in Figure 1.2(a). This is a two-dimensional representation of the crystal lattice. The entire lattice can be constructed by translations of any of the three unit cells in two coordinate directions. The primitive unit cell is the smallest unit cell. A generalised primitive three-dimensional unit cell is shown in Figure 1.2(b). The coordinate directions are **a,b,c**. In cubic structures, these would be the rectangular coordinates. The basic cubic crystal structures are (a) the simple cubic, (b) the body-centred cubic and

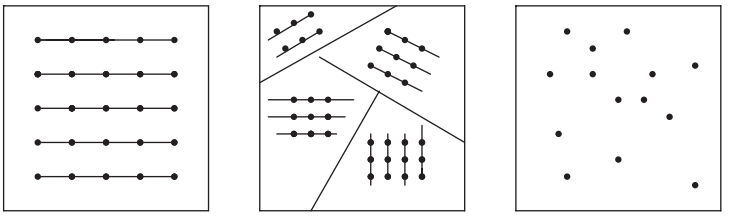

(a) Crystalline (b) Polycrystalline (c) Amorphous

Fig. 1.1 Schematic arrangement of atoms in solids.

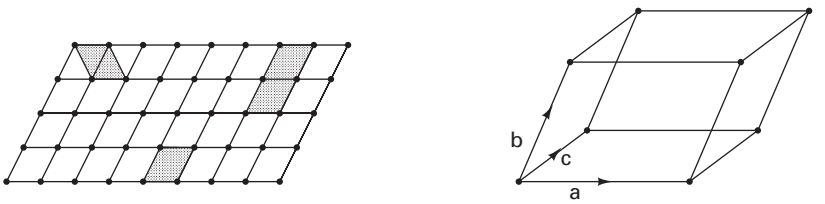

(a) Two-dimensional lattice – shaded areas show possible unit cells

(b) Generalised primitive unit cell

Fig. 1.2 Unit cells.

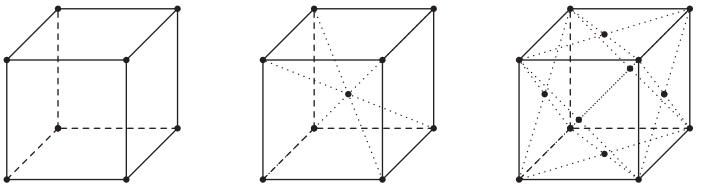

(a) Simple cubic (b) Body-centred cubic (c) Face-centred cubic

Fig. 1.3 Types of cubic lattices.

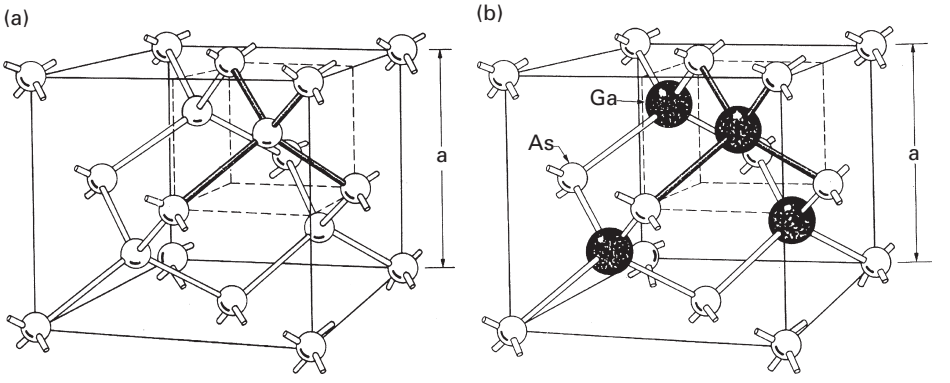

Fig. 1.4 (a) Diamond lattice and (b) Zincblende lattice. (S. M. Sze, *Semiconductor Devices: Physics and Technology*, John Wiley & Sons, 1985). Reprinted with permission of John Wiley & Sons, Inc.

(c) the face-centred cubic shown in Figure 1.3. The simple cubic lattice has an atom at each corner of the cube, where the length of a side of the cube is a, the lattice constant. The body-centred cubic lattice (BCC) has an additional atom in the centre of the cube and the face-centred cubic lattice (FCC) has an additional atom in the centre of each face of the cube. The two most important semiconductor crystal structures are the diamond lattice structure and the zincblende structure. Silicon and germanium have the diamond lattice structure and most of the binary compound semiconductors such as GaAs have the zincblende lattice structure. The only difference between the diamond and the zincblende structures is that the latter has two different types of atoms as seen in Figure 1.4. The diamond structure consists of two inter-penetrating FCC sublattices of atoms. The second FCC cube is shifted by one-fourth of the body diagonal, which is the longest diagonal. In the zincblende structure of GaAs, one sublattice has gallium atoms and the other has arsenic atoms.

1.5 Crystal directions and planes

Crystals are of finite size and hence have surfaces. It is necessary to define the planes at the crystal surfaces and the crystallographic directions, both of which determine the

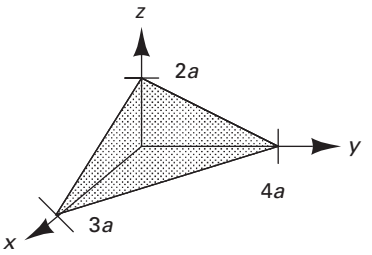

Fig. 1.5 Representation of plane with Miller indices [6, 5, 8].

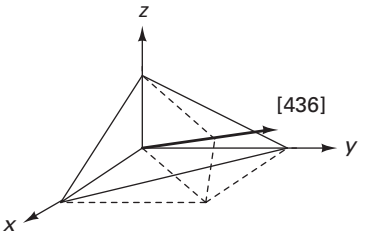

Fig. 1.6 Representation of direction with Miller indices [6, 5, 8].

properties of semiconductor devices. The rectangular coordinate system defines the cubic crystal and the plane surfaces and directions are described by a set of indices called the *Miller indices*. Planes are described by the indices (h,k,l) and the directions perpendicular to these planes are described by the same indices [hkl].

Example: Find the Miller indices of the plane which makes intercepts $3a$,$4a$,$2a$ along the coordinate axes in a cubic crystal, where a is the lattice constant. Draw the direction vector with the same Miller indices.

Solution: The intercepts are 3, 4 and 2. The reciprocals are 1/3, 1/4 and 1/2. Multiplication by the lowest common denominator, which is 12, yields (4,3,6). These are the Miller indices which define the plane shown in Figure 1.5. It can be shown that parallel planes are described by the same Miller indices.

The Miller indices of the direction are given as [436]. The intercepts on the three coordinate axes are 3, 4 and 2. The direction vector is drawn and seen to be perpendicular to the planes shown in Figure 1.6.

The basic planes in cubic crystals are shown in Figure 1.7. It is also important to describe specific directions in a crystal in addition to the planes. As in the case of the crystal plane, a crystal direction is also described by three integers which are the components of a vector drawn in the particular crystal direction. The crystal planes and directions of most interest are shown in Figure 1.8. The [hkl] direction is perpendicular to the (hkl) plane.

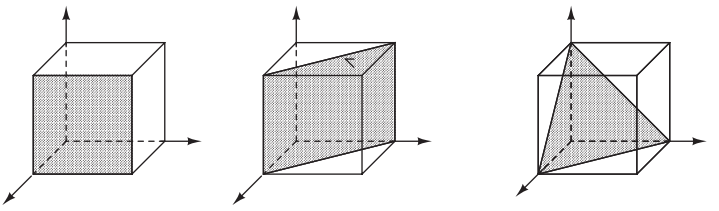

Fig. 1.7 Basic crystal planes.

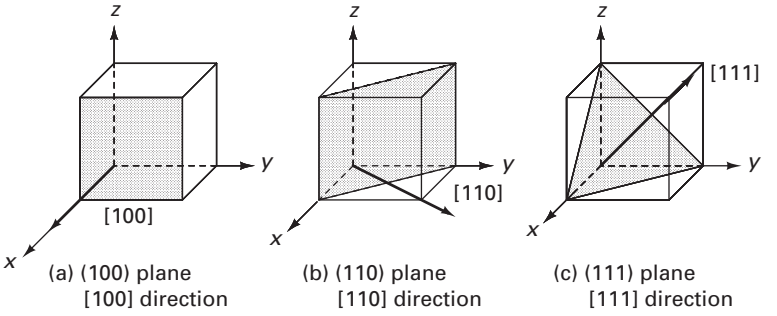

Fig. 1.8 Important crystal planes and directions.

1.6 Atomic bonding

Atoms are held together by bonding forces to form solids. When the attractive and repulsive forces are equivalent, the atoms are in equilibrium and maintain the spacing characterised by the lattice constant, a. There are different bonding classifications which are described by the dominant force of attraction. When one of the atoms gives up an electron in the outer shell to another atom, positive and negative ions are produced. There is a Coulomb interaction force of attraction between them. This is termed *ionic bonding*. At equilibrium, the forces of attraction and repulsion are equivalent. Sodium chloride (NaCl) and Potassium chloride (KCl) are examples of ionic bonding after the formation of the Na^+ and Cl^- ions.

1.6.1 Covalent bonding

This type of bonding results when electrons are shared by neighbouring atoms. The hydrogen atom is the simplest example of covalent bonding. Each of the two electrons bonds with the other to complete the lowest energy shell as shown in Figure 1.9.

Each atom in a diamond or zincblende lattice has four nearest neighbours. Each atom has four electrons in the outer orbit. These are the valence electrons and each atom shares these valence electrons with its four neighbours. The interaction between the shared electrons results in bonding forces which are quantum mechanical in nature. In other words, each electron pair constitutes a covalent bond. Elements in group IV such as Si and Ge have four valence electrons as shown in the references [8, 14, 15]. These are available for bonding as seen in Figure 1.10. Compound semiconductors such as

Fig. 1.9 Covalent bonding in hydrogen.

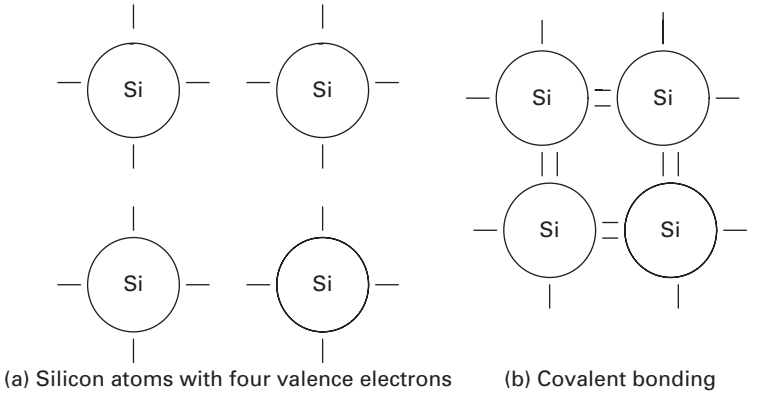

Fig. 1.10 Covalent bonding in silicon.

GaAs exhibit both covalent as well as ionic bonding. This is due to the fact that Ga and As occur in two different groups in the periodic table and hence there is a transfer of charge resulting in some ionic bonding.

1.7 Atomic physics

The theories of atomic physics were based on experimental observations. These theories subsequently explained the experiments and led to the understanding of atoms in matter.

1.7.1 The photoelectric effect

The measurements of Planck on a heated sample of material indicated that energy is radiated in discrete units called *quanta* as shown in Equation (1.1).

$$E = h\nu, \tag{1.1}$$

where h (Planck's constant) $= 6.63 \times 10^{-34}$ J · s and ν is the frequency of the radiation. Heinrich Hertz discovered the photoelectric effect in 1887. The experiments performed by Philipp Lenard, a former student of Hertz, showed that if light shines on a metal surface in vacuum, some of the electrons receive enough energy so that they are emitted from the surface into the vacuum. They were interpreted by Albert Einstein, who received the Nobel Prize for his work in 1921. This is termed the *photoelectric effect* and the maximum energy is a function of the frequency of the incident light. The quantised units of light energy are called *photons*.

Based on further experimental observations of Davisson and Germer (USA) and Thompson (UK) on the diffraction of electrons by the atoms in a crystal, de Broglie related the wavelength of a particle of momentum $p = mv$, where m is the mass of the particle as seen in Equation (1.2):

$$\lambda = \frac{h}{p} = \frac{h}{mv}. \tag{1.2}$$

1.7.2 The Bohr model of the atom

A model of the atom was first proposed by Bohr. In his model, the electrons move in stable circular orbits about the nucleus and the electron may move to an orbit of higher or lower energy. The electron would either gain energy or lose energy by the absorption or emission of a photon of energy $h\nu$. Bohr further proposed that the angular momentum of the electron moving in a circular orbit was an integral multiple of Planck's constant as seen in Equation (1.3).

$$p_\theta = \frac{nh}{2\pi} = n\hbar, \; n = 1, 2, 3, \ldots \tag{1.3}$$

The hydrogen atom with one electron and the nucleus illustrates this concept in a simple manner as seen in Figure 1.11.

Assuming that the electron of mass m rotates in a stable orbit of radius r with velocity v, the angular momentum is written in Equation (1.4):

$$p_\theta = mvr = n\hbar. \tag{1.4}$$

The electrostatic force between the charge on the nucleus and the charge on the electron must be equal to the centripetal force for the electron to remain in stable orbits. This yields the expression in Equation (1.5) for the energy of the electron [15]:

$$E_n = -\frac{mq^4}{2(4\pi\epsilon_0)^2 n^2 \hbar^2}. \tag{1.5}$$

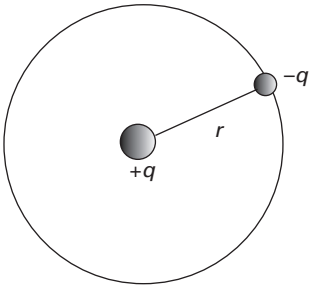

Fig. 1.11 Bohr model of the hydrogen atom.

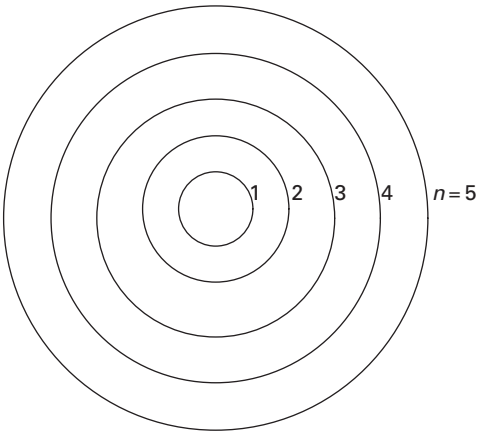

Fig. 1.12 Electron orbits in Bohr model (not to scale).

The electron orbits in the Bohr model are shown in Figure 1.12.

1.8 The de Broglie relation

The initial theoretical and experimental results of Planck, Einstein and Bohr laid the foundation for the development of quantum mechanics. It was de Broglie, however, who first postulated that if waves were seen to behave as particles then it could be that particles might behave like waves.

In the Bohr formulation, the electron which travels in a circular orbit of radius r is assumed to behave like a wave with a wavelength λ. It travels in a circular path equal in length to the circumference $2\pi r$, which will be an integral number of wavelengths so that

$$n\lambda = 2\pi r. \tag{1.6}$$

The Bohr formulation yielded the linear velocity of the electron to be

$$v = \frac{q^2}{4\pi\epsilon_0 n\hbar}. \tag{1.7}$$

Using this velocity relation, the wavelength can be written as

$$\lambda = \frac{h}{mv} = \frac{h}{p}, \tag{1.8}$$

where p is the linear momentum of the electron. Thus, de Broglie postulated that the relationship between the wavelength and the linear momentum p of a particle is given by Equation (1.2).

$$p = \frac{h}{\lambda} = \frac{h}{2\pi}\frac{2\pi}{\lambda} = \hbar k. \tag{1.9}$$

This is the *de Broglie relationship*. For free electrons, the energy–momentum relationship is as follows:

$$E = \frac{mv^2}{2} = \frac{p^2}{2m};\ p = \sqrt{2mE}. \tag{1.10}$$

Hence, the experiments of Davisson and Germer and of Thompson were verified by the de Broglie relationship.

1.9 Quantum mechanics

Newtonian mechanics can be used to describe physical behaviour that is macroscopic. Typical examples of this are planetary motion, the classical electromagnetic fields and fluid motion. The motion of electrons and the interaction of electrons in atoms in semiconductor materials cannot, however, be described thus since we are dealing with microscopic behaviour. This physical behaviour on the atomic scale can only be described by quantum mechanics rather than Newtonian mechanics. Quantum or wave mechanics had as its basis the physical understanding developed by Planck and de Broglie. The classical laws of the conservation of energy, momentum and angular momentum are also assumed to be valid in quantum mechanics. Hence, the physics involved in the interaction between atoms can be described mathematically by quantum mechanics.

1.9.1 Probability and the uncertainty principle

When the motion of the particle is microscopic, the parameters cannot be described exactly but rather in terms of average (expectation) values. Hence we have, for example, the expectation values of position, momentum and energy of an electron. So, we have a probabilistic rather than an exact description of the particle behaviour. There is, thus, an inherent uncertainty in the position and momentum of the particle. This was formulated by Heisenberg and is termed the *Heisenberg uncertainty principle*. The uncertainty in the measurement of the position and momentum of particle motion is given as

$$(\Delta x)(\Delta p_x) \geq \hbar. \tag{1.11}$$

The uncertainty in energy is related to the time at which the energy was measured and is given by

$$(\Delta E)(\Delta t) \geq \hbar. \tag{1.12}$$

These equations show that the simultaneous measurements of position and momentum on the one hand and energy and time on the other hand cannot be performed with arbitrary accuracy.

It follows that we can only determine the probability of finding an electron in a certain position or having a certain momentum. This leads to the definition of a probability density function. The probability of finding a particle in a range, say, from x to $x + dx$ is given by

Table 1.4 Classical variables and quantum operators

Classical variable	Quantum operator
x	x
$f(x)$	$f(x)$
Momentum $p(x)$	$\frac{\hbar}{j}\frac{\partial}{\partial x}$
Kinetic energy $\frac{p^2}{2m}$	$\frac{-\hbar^2}{2m}\frac{\partial^2}{\partial x^2}$
Potential energy V	V
Total energy E	$\frac{-\hbar}{j}\frac{\partial}{\partial t}$

$$\int_{-\infty}^{\infty} P(x)dx = 1, \tag{1.13}$$

where $P(x)$ is a normalised function. The average value of a function x is defined as

$$\langle f(x)\rangle = \int_{-\infty}^{\infty} f(x)P(x)dx = 1. \tag{1.14}$$

The correspondence between classical and quantum mechanical quantities is shown in Table 1.4.

The basic principles of quantum mechanics will now be reviewed. Each particle in a physical system is described by a wave function $\Psi(x, y, z, t)$. The function and its space derivatives are continuous, finite and single-valued.

The probability of finding a particle with wave function Ψ in the volume $dxdydz$ is $\Psi^*\Psi dxdydz$. Then we have the following definition for three-dimensional space:

$$\int_{-\infty}^{\infty} \Psi^*\Psi dxdydz = 1. \tag{1.15}$$

The expectation value of any physical quantity X can be written as

$$< X > = \int_{-\infty}^{\infty} \Psi^* X_{\text{oper}} \Psi dxdydz, \tag{1.16}$$

where X_{oper} is the operator corresponding to the variable X.

The classical equation for energy conservation is Kinetic energy + Potential energy = Total energy:

$$\frac{p^2}{2m} + V = E. \tag{1.17}$$

1.9.2 The wave equation

We obtain the quantum mechanical energy equation by substituting the corresponding operators which operate on the one-dimensional wave function $\Psi(x, t)$:

$$\frac{-\hbar^2}{2m}\frac{\partial^2\Psi(x,t)}{\partial x^2} + V(x)\Psi(x,t) = E\Psi(x,t) = \frac{-\hbar}{j}\frac{\partial\Psi(x,t)}{\partial t}. \tag{1.18}$$

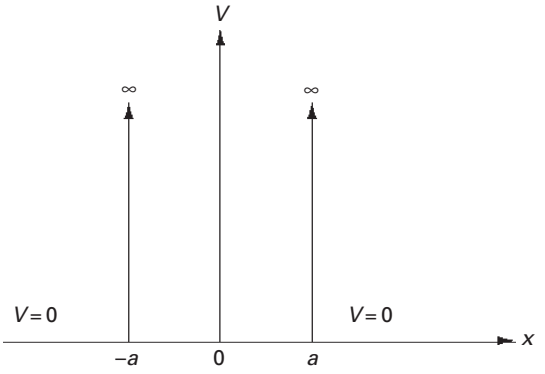

Fig. 1.13 Infinite potential well, width = $2a$.

This is the one-dimensional Schrödinger wave equation. The three-dimensional wave equation is

$$\frac{-\hbar^2}{2m}\nabla^2\Psi + V(x)\Psi = E\Psi = \frac{-\hbar}{j}\frac{\partial\Psi}{\partial t}. \tag{1.19}$$

The wave equation is applied to the solution of various physical problems. The problem of the infinite potential well provides an understanding of the method of solution and an insight into the discrete energies of a single electron [14, 15].

This basic physical concept is important since quantum wells can be fabricated using semiconductor structures for devices. A general solution of the one-dimensional wave equation can be written as follows:

$$\Psi(x,t) = \psi(x)\exp\left(\frac{-jEt}{\hbar}\right). \tag{1.20}$$

We consider the infinite quantum well of width $2a$ with zero potential outside the well as shown in Figure 1.13.

On solving the one-dimensional wave function, we obtain n solutions and the discrete energy levels are given by [14, 15],

$$E_n = \frac{\pi^2\hbar^2 n^2}{8m_0a^2}, \tag{1.21}$$

where m_0 is the rest mass of the electron and a is the lattice constant of the crystal. The one-dimensional problem of a particle in a finite potential well can also be solved and the allowed energies of the particle determined [10]. The phenomenon of tunnelling wherein an electron with energy E tunnels through a potential barrier with barrier height V_0 greater than E is also explained by quantum mechanics. Classically, the electron would not be able to show this behaviour. If we have a potential barrier of width a, the one-dimensional Schrödinger equation can be solved in the three regions I, II and III as

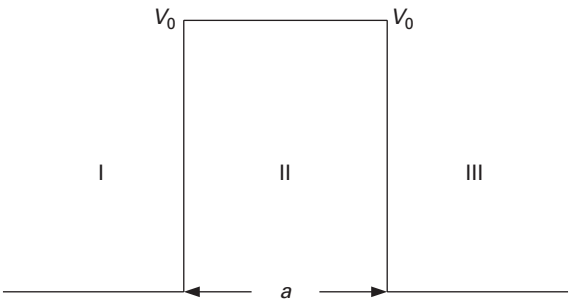

Fig. 1.14 Potential barrier.

shown in Figure 1.14. There are three regions for the problem. Regions I and III have zero potential. Say region II has a potential V_0, then the solutions in the three regions are given by:

$$Region\ \ I\colon \psi(x) = A\exp(jkx) + B\exp(-jkx);\ k^2 = \frac{2mE}{\hbar^2} \tag{1.22}$$

$$Region\ \ II\colon \psi(x) = C\exp(-\alpha x) + D\exp(+\alpha x);\ \ \alpha^2 = \frac{2m(V_0 - E)}{\hbar^2} \tag{1.23}$$

$$Region\ \ III\colon \psi(x) = F\exp(jkx);\ \ k^2 = \frac{2mE}{\hbar^2}. \tag{1.24}$$

Using the conditions that the wave function and its derivatives are continuous at the boundaries, $x = 0$ and $x = a$, the tunnelling probability is of the form:

$$T = \left|\frac{F}{A}\right|^2 = \frac{4}{4\cosh^2(\alpha d) + \left(\frac{\alpha}{k} - \frac{k}{\alpha}\right)^2 \sinh^2(\alpha d)}. \tag{1.25}$$

Boundary conditions are matched at the two boundaries and T, the tunnelling probability is determined.

The method of solution is the same regardless of the shape of the barrier. Triangular and trapezoidal barriers have a simple geometry and hence give us exact solutions. When the barriers are of arbitrary shape, the tunnelling probability is solved using the Wentzel–Kramers–Brillouin (WKB) approximation:

$$T \cong \exp\left[-2\int_{d_1}^{d_2} |\ f(x)\ |\ dx\right] \tag{1.26}$$

with

$$f(x) = \frac{2m_0}{\hbar^2}[V(x) - E], \tag{1.27}$$

where $V(x)$ is the arbitrary potential. The limits of the integral d_1 to d_2 represent the classically forbidden region, where the potential energy is larger than the total particle energy.

1.10 Statistical mechanics

1.10.1 The free electron

When the three-dimensional Schrödinger equation is solved, the general solution gives the wave function for the electron in motion in a region of zero potential. The behaviour of electrons in semiconductor crystals can be assumed to be like that of so-called *free electrons* under certain conditions, hence the importance of this result. The time-independent wave function solution is given by

$$\psi(\mathbf{r}) = \mathbf{A}\exp(\mathbf{k}\cdot\mathbf{r}), \tag{1.28}$$

where $\mathbf{A}$ is a complex quantity and is the amplitude, $\mathbf{k}$ is the wave vector and $\mathbf{r}$ is the three-dimensional space vector. This results in energies of the same form as Equation (1.21).

1.10.2 Fermi–Dirac distribution

The Fermi–Dirac distribution function $f(E)$ gives the probability that states with energy E are occupied by particles [10]:

$$f(E) = \frac{1}{1+\exp\left(\frac{E-E_{\mathrm{F}}}{kT}\right)}, \tag{1.29}$$

E_{F} represents the Fermi energy where f(E) becomes equal to 1/2.

1.11 Electrons in a semiconductor

Since semiconductors have periodic lattice structures, the electrons are subjected to a periodic potential. Hence the Schrödinger equation must be solved for a periodic potential [10]. The *Bloch theorem* states that the one-dimensional wave function for an electron in a periodic potential is given by

$$\psi(x) = V_{\mathrm{k}}(x)\exp(jkx), \tag{1.30}$$

where $V_{\mathrm{k}}(x)$ is a periodic potential with the same periodicity as the semiconductor crystal with lattice constant a such that

$$V_{\mathrm{k}}(x) = V_{\mathrm{k}}(x+na), \tag{1.31}$$

where n is an integer.

1.12 The Kronig–Penney model

An important model for the band structure is the Kronig–Penney model (Figure 1.15).

The one-dimensional periodic potential is given by

$$V(x) = 0,\ 0 \le x \le a \tag{1.32}$$

$$V(x) = V_0,\ -b \le x \le 0 \tag{1.33}$$

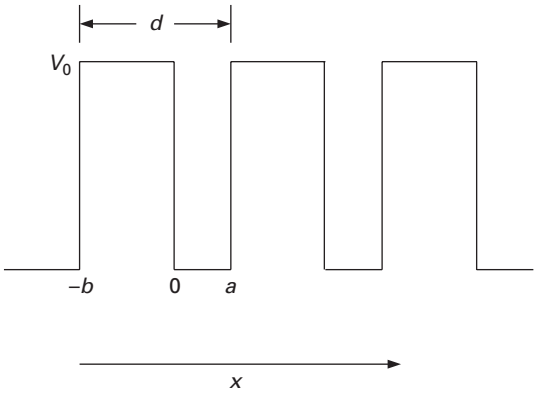

Fig. 1.15 Periodic potential for Kronig–Penney model.

The periodicity distance is $d = a + b$. The wave equation is solved in the three regions and the continuity conditions for the wave function and its derivatives are applied. The non-trivial solutions are obtained when the electron energy is less than and greater than the potential V_0 [10, 14]. The transcendental equation to be solved is

$$\cos k_x d = \cos a\alpha \cosh\, b\delta - \frac{\alpha^2 - \delta^2}{2\alpha\delta} \sin a\alpha \sinh\, b\delta,\ 0 < E < V_0 \tag{1.34}$$

$$\cos k_x d = \cos a\alpha \cos b\delta - \frac{\alpha^2 + \delta^2}{2\alpha\delta} \sin a\alpha \sin b\delta,\ E > V_0 \tag{1.35}$$

with

$$\alpha = \sqrt{\frac{2m_0 E}{\hbar^2}},\ \beta = \sqrt{\frac{2m_0(E - V_0)}{\hbar^2}}, \delta = \sqrt{\frac{2m_0(V_0 - E)}{\hbar^2}}. \tag{1.36}$$

The solution of the equation gives the energy E. The allowed energy bands are separated by band gaps with no allowed energies. It follows that there are forbidden energy regions for an electron which is subjected to a periodic potential in a semiconductor crystal.

1.12.1 Effective mass

When the centre of mass of a classical particle moves with a velocity v, we define a phase velocity. If we have a packet of travelling waves with a centre frequency ω and a wavenumber k, we have the classical dispersion relation for the group velocity:

$$v_g = \frac{d\omega}{dk}. \tag{1.37}$$

In the quantum mechanical formulation, the wavepacket is the analogue of the classical particle in a given region of space. This wavepacket consists of constant-energy wave

function solutions and a centre energy is defined. Hence the wavepacket group velocity in the quantum-mechanical formulation can be written as in Equation (1.20):

$$v_g = \frac{1}{\hbar}\frac{dE}{dk}. \tag{1.38}$$

Using the force–momentum relations, we define the effective mass of an electron in a crystal as

$$m^* = \left(\frac{1}{\hbar^2}\frac{d^2E}{dk^2}\right)^{-1}. \tag{1.39}$$

Section 1.14.1 defines heavy and light holes corresponding to wide and narrow bands respectively.

1.12.2 Carriers in semiconductors

The two types of carriers in semiconductors are the conduction band electrons and the valence band holes. The electrons occupy the conduction band when the temperature is raised above 0 K. The unoccupied states in the valence band are holes and are defined to have a positive charge with the same magnitude as the electronic charge. Hence, we consider electrons in determining the conduction band properties and holes in determining the valence band properties. The band structures of several semiconductors are given by Pierret, and Streetman and Banerjee [10, 15] and others.

1.13 Semiconductors in equilibrium

1.13.1 Intrinsic semiconductors

A semiconductor is described as being intrinsic when there are no impurities and no defects in the crystal. The concentration of electrons in the conduction band is equal to the concentration of holes in the valence band. At 0 K, the electrons occupy all the available energy states in the valence band and all the states in the conduction band are empty. This follows from the fact that at 0 K, each electron is in the lowest possible energy state. As the temperature is increased the electrons are excited due to the acquired thermal energy and move into the conduction band leaving behind holes in the valence band. Therefore, the equilibrium concentration of electrons in the conduction band n_0 is equal to the equilibrium concentration of holes in the valence band p_0 in intrinsic semiconductors [2, 15]:

$$n_0 = p_0 = n_i, \tag{1.40}$$

where n_i is simply referred to as the intrinsic concentration of holes and electrons.

1.13.2 Extrinsic semiconductors

When impurity atoms are added to the intrinsic semiconductor such that the electron concentration is no longer equal to the hole concentration, it becomes an extrinsic

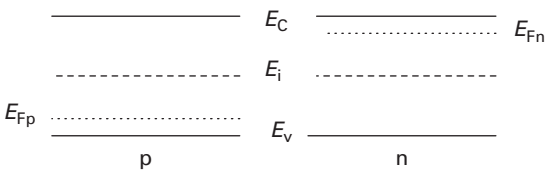

Fig. 1.16 Band diagram.

semiconductor and $n_0 \neq p_0$. Thus the doping of a semiconductor with impurities can produce excess electrons or holes. These atoms can be either donors or acceptors. If the dopant produces an excess of electrons, the dopant is referred to as a *donor*, the semiconductor becomes n-type material with $n > p$ and the current is predominantly due to the negatively charged electrons. If, on the other hand, the dopant generates holes, the dopant is referred to as an *acceptor*, the result is a p-type semiconductor with $p > n$ and the current is predominantly due to the positively charged holes. Note that the hole charge has the same magnitude as the electronic charge [2, 8, 15].

1.13.3 Semiconductor band diagrams

The band diagrams for p- and n-type semiconductors at thermal equilibrium are given in Figure 1.16. The bottom of the conduction band is E_c, the top of the valence band is E_v, the intrinsic energy level is at mid-band and is denoted by E_i and the Fermi level is E_F.

1.13.4 Electron and hole distribution

The distribution of electrons in the conduction band and holes in the valence band is obtained using the Fermi–Dirac probability function. The electron distribution in the conduction band is written as

$$n(E) = g_c(E) f(E), \tag{1.41}$$

where $g_c(E)$ is the density of quantum states in the conduction band and $f(E)$ is the Fermi–Dirac probability function given in Equation (1.29). The hole distribution in the valence band can be written in a similar way:

$$p(E) = g_v(E)[1 - f(E)]. \tag{1.42}$$

The density of states functions are written as

$$g_c(E) = \frac{m_n^* \sqrt{2m_n^*(E - E_c)}}{\pi^2 \hbar^3}, \quad E \geq E_c \tag{1.43}$$

$$g_v(E) = \frac{m_p^* \sqrt{2m_p^*(E_v - E)}}{\pi^2 \hbar^3}, \quad E \leq E_v. \tag{1.44}$$

The equilibrium concentration of electrons can now be written as

$$n_0 = \int_{E_c}^{\infty} n(E) \mathrm{d}E, \tag{1.45}$$

where $n(E)$ is given by Equation (1.41). Similarly, the equilibrium hole concentration is written as

$$p_0 = \int_{-\infty}^{E_v} p(E)\mathrm{d}E, \tag{1.46}$$

where $p(E)$ is given by Equation (1.42). The equilibrium electron and hole concentrations in the conduction and valence bands respectively are written as

$$n_0 = N_c \exp\left(\frac{-(E_c - E_F)}{kT}\right) \tag{1.47}$$

$$p_0 = N_v \exp\left(\frac{-(E_F - E_v)}{kT}\right), \tag{1.48}$$

where N_c and N_v are the effective density of states functions in the conduction and valence bands respectively.

$$N_c = 2\left(\frac{2\pi m_n^* kT}{h^2}\right)^{3/2} \tag{1.49}$$

$$N_v = 2\left(\frac{2\pi m_p^* kT}{h^2}\right)^{3/2}. \tag{1.50}$$

The intrinsic carrier concentration n_i is given by

$$n_i^2 = n_0 p_0. \tag{1.51}$$

By substitution of Equations (1.47) and (1.48), we can write the intrinsic concentration as

$$n_i^2 = N_c N_v \exp\left(\frac{-(E_c - E_v)}{kT}\right) \tag{1.52}$$

$$= N_c N_v \exp\frac{-E_g}{kT}, \tag{1.53}$$

where E_g is the bandgap energy.

1.14 Direct and indirect semiconductors

When light illuminates a semiconductor, and the photon energy is equal to or larger than the band gap, the light is absorbed, and creates hole–electron pairs. These holes and electrons are equal in number to maintain charge neutrality, and since they are not in equilibrium, in due course they recombine; this recombination may be radiative or non-radiative. Radiative recombination, when a photon is emitted usually at the bandgap energy, only occurs in direct bandgap material, whereas non-radiative recombination may occur in both direct and indirect bandgap semiconductors. In indirect semiconductors, this non-radiative recombination requires a phonon to mediate the process. Non-radiative processes in direct bandgap material are usually through traps or due to surface recombination. The direct or indirect band gap defines whether the lowest

position of the conduction band aligns with the maximum of the valence band along momentum space, where the effective momentum value k is equal to zero.

Direct bandgap semiconductors are capable of photon emission, by radiative recombination, but indirect semiconductors have a low probability of radiative recombination. However, indirect bandgap semiconductors may have isoelectronic impurity states which are direct, and therefore the recombination from these states may also be radiative. GaP, which is an indirect gap semiconductor, may be doped with zinc oxide or nitrogen to produce these states, and the widely used green or red light–emitting diodes are examples of this emission.

1.14.1 Absorption processes

Considering Figure 1.17, we note that three different valence bands are shown. Equation (1.39) had linked the carrier mobility the second derivative of energy with respect to k. It is then easy to understand why the band with less curvature at $k = 0$ (V_1) is called the "heavy hole band", while the one which is more strongly bent (V_2) is called "light hole band". In most bulk semiconductors, the light and heavy hole bands concide at $k = 0$ – they are degenerate. The band V_3 is called the "split-off band". Note

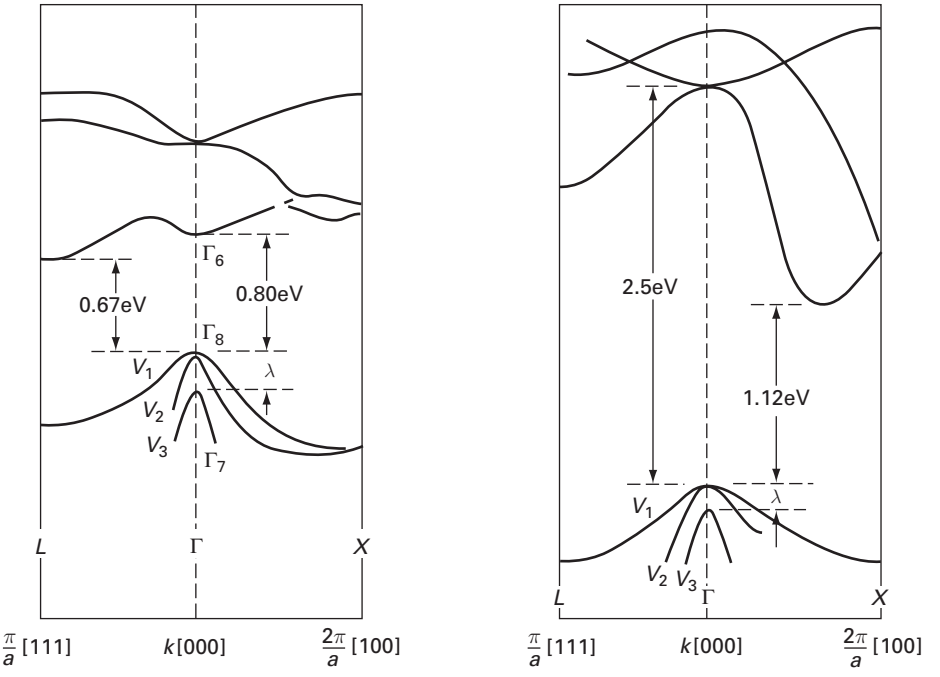

Fig. 1.17 Band diagram of bulk Ge (left) and Si (right). Note that the minimum of the conduction band is not aligned with maximum of the valence band at $k = 0$, indicating that these are indirect semiconductors. S. Wang, *Fundamentals of Semiconductor Theory and Device Physics*, 1st Edition, pp. 233–234, ©1989. Reprinted by permission of Pearson Education, Inc., Upper Saddle River, NJ.

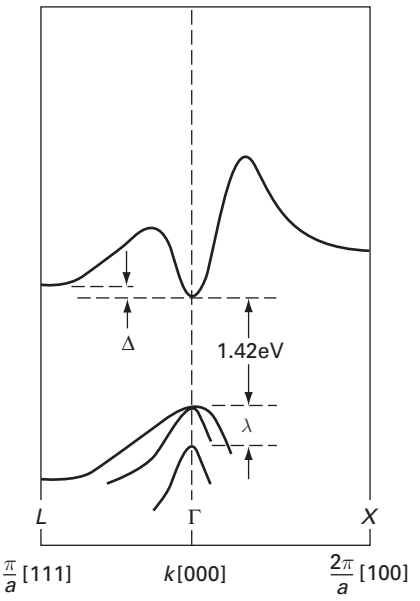

Fig. 1.18 Band diagram of bulk GaAs. Note that the minimum of the conduction band is aligned with maximum of the valence band at $k = 0$, indicating that this is a direct gap semiconductor.
S. Wang, *Fundamentals of Semiconductor Theory and Device Physics*, 1st Edition, pp. 233–234, ©1989. Reprinted by permission of Pearson Education Inc., Upper Saddle River, NJ.

that in each of these cases, the minimum of the conduction band is not aligned with the maximum of the valence band where $k = 0$, which implies that these are indirect semiconductors. In Figure 1.18, the band diagram of the direct semiconductor GaAs is shown; here the conduction band minimum is along the $k = 0$ axis and aligned with the maximum of the valence band. Note the degenerate valence band of heavy holes and light holes and the split-off band.

Photo-excitation of semiconductors with photons energies equal to or greater than the bandgap energy of the material results in absorption, which in turn causes the creation of hole–electron pairs for each photon. The major source of absorption in semiconductors is the valence band to conduction band transition. In the case of direct semiconductors, the transition occurs when the photon energy is at the bandgap value or larger and results in the transition of an electron in the valence band to the conduction band. In indirect semiconductors, the absorption has to be mediated by phonons. In addition to the band to band absorption, transitions take place from acceptor to donor levels, from acceptor to conduction band, valence to donor level, all of which result in absorption below the bandgap energy. Figure 1.19 shows schematically the band to band transition for the direct gap semiconductor, and in Figure 1.20, the phonon-mediated transition. The conduction band to valence band and impurity band to impurity band transitions are shown schematically in Figure 1.21. Not shown in this figure are the impurity band to conduction and valence band transitions, all of which lead to absorption and emission of the appropriate photon energies.

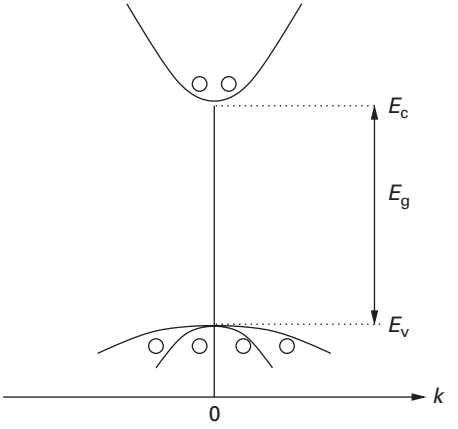

Fig. 1.19 Schematic diagram of the conduction and valence bands of a direct semiconductor and the transitions.

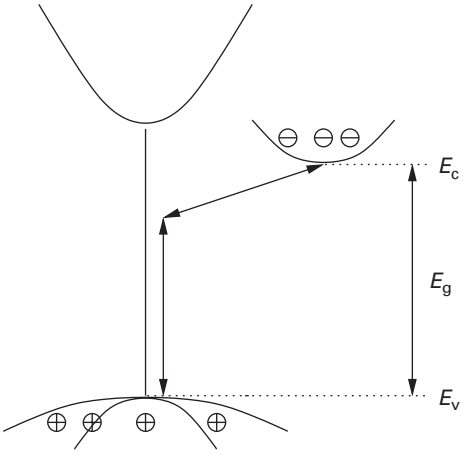

Fig. 1.20 Schematic diagram of the indirect semiconductor and the phonon-mediated transitions.

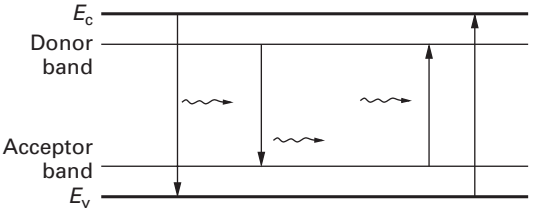

Fig. 1.21 Transitions possible with a semiconductor with impurity donor and acceptor bands: conduction band to valence band and impurity band to impurity band are illustrated. Others, conduction band to impurity band and valence band to impurity band have not been shown.

The absorption rate of the band to band transitions, for both the direct and indirect transitions may be calculated using quantum theory, but is not included here.

Free carrier absorption also occurs in most semiconductors as the carrier density is always non-zero. The absorption of a photon by a carrier within a band results in the carrier having a larger energy. The absorption coefficient is proportional to the carrier density [3]. This effect is important in the design of waveguide devices, where typically this may result in absorption of the order of 1 dB cm^{-1} when the carrier densities are high in the 10^{18} cm^{-3} region.

1.14.2 Exciton absorption

In pure semiconductors, the absorbed photon with bandgap energy or larger may create excitons, which are electron–hole pairs that are bound, and in the binding process give up the binding energy. The binding energy of these excitons is of the order of about 4.5 meV, and at low temperatures, an excitonic absorption peak is seen a little below the band to band absorption energy. At room temperature, this peak is not seen in bulk material, because the thermal broadening due to optical phonons is comparable, and the excitons that are created dissociate very rapidly. In quantum wells, however, the excitons remain extant at room temperature due to enhanced binding energies, which are typically two or three times that of the thermal broadening energy. Thus, the absorption characteristics of the material with quantum wells also show the excitonic absorption in addition to the usual band to band absorption. When a transverse electric field is applied to the quantum well, the absorption edge shifts to a longer wavelength. A simple explanation of this phenomenon is shown in Figure 1.22, where the schematic wave functions of the electron and hole in the quantum well are shown. When the transverse field is applied, then the quantum well bands tilt, and the resulting gap between the electron–hole wave functions decreases, which results in the absorption edge moving to a smaller energy and thus a longer wavelength.

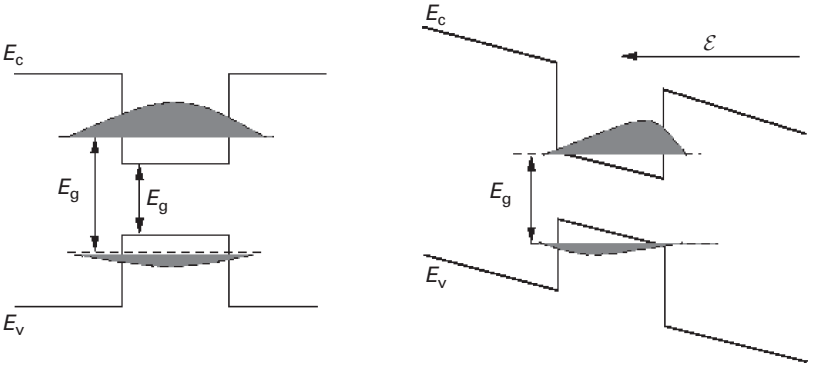

Fig. 1.22 A schematic diagram of the wave functions in a quantum well, and the effect of applying a field across the well, resulting in tilting of the wells. This so-called Quantum Confined Stark Effect reduces the effective band gap of the material.

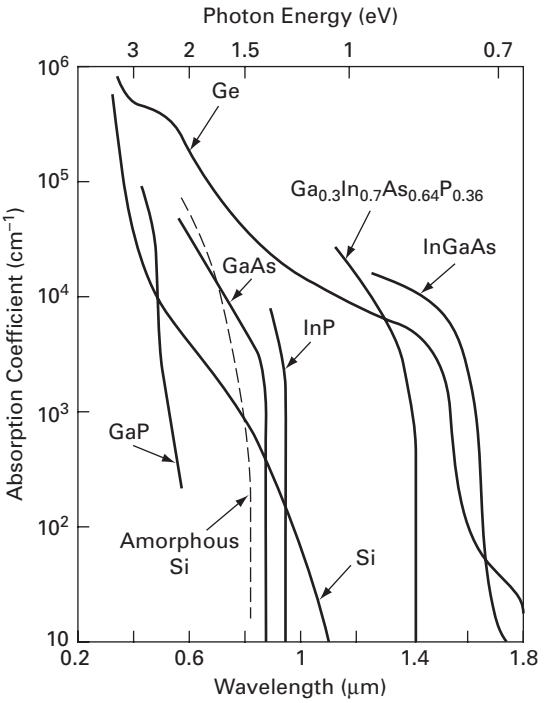

Fig. 1.23 Absorption coefficient for various semiconductors (M. Shur, *Physics of Semiconductor Devices*, Prentice Hall, 1990 ©Prentice Hall).

Other absorption mechanisms are due to valence to impurity band, impurity band to other impurity band or impurity band to conduction band transition, intraband absorption between different levels in the same band, and free carrier absorption.

The absorption spectra of different semiconductors is summarised in Figure 1.23.

1.15 Recombination and radiation in semiconductors

The absorption of photons by the semiconductor results in the generation of electrons and holes, which disturbs the equilibrium status of the semiconductor. Electrical injection also results in this non-equilibrium of an excess of electrons in the conduction band and an equal number of holes in the valence band. These recombine, both non-radiatively and radiatively, the latter in direct gap semiconductors. In general, the radiative transitions are dominated by the conduction band to valence band emission and therefore define the energy of the emitted photons. Other recombination processes include exciton recombination, donor to acceptor and other impurity recombinations. The radiation spectrum from recombination is generally shifted to lower energy from the absorption spectrum, and this is termed the *Stokes* or the *Franck–Condon shift* due to imperfections in materials or interfaces.

In general the excess electrons and holes decay at some rate, resulting in the density varying as $\exp(-t/\tau)$, where τ is defined as the lifetime of the carriers. The decay of these carriers results in transfer of energy to the lattice in the form of phonons for the non-radiative decay and transfer of energy to photons for radiative decay.

The corresponding lifetimes are labelled as τ_{nr} and τ_r for the non-radiative and radiative decay, respectively, and the corresponding non-radiative and radiative rates are R_{nr} and R_r, respectively. Thus, the total lifetime constant τ is given as:

$$\frac{1}{\tau} = \frac{1}{\tau_{nr}} + \frac{1}{\tau_r}. \tag{1.54}$$

The corresponding total spontaneous rate of recombination is given by

$$R_{spon} = R_{nr} + R_r. \tag{1.55}$$

Devices such as the light-emitting diode (LED) largely depend on spontaneous emission, and in this case the internal quantum efficiency is given by

$$\eta_{internal} = \frac{R_r}{R_{nr} + R_r}. \tag{1.56}$$

The exponential decay rate of the excess carriers is inversely proportional to recombination rate, and if the excess of electron is Δn, then the recombination rates R_r and R_{nr} are given by the expressions: $R_r = \Delta n/\tau_r$ and $R_{nr} = \Delta n/\tau_{nr}$. Then internal quantum efficiency may also be written as

$$\eta_{internal} = \frac{\frac{1}{\tau_r}}{\frac{1}{\tau_r} + \frac{1}{\tau_{nr}}} = \frac{1}{1 + \frac{\tau_r}{\tau_{nr}}} = \frac{\tau_{nr}}{\tau_r + \tau_{nr}}. \tag{1.57}$$

The total spontaneous recombination rate is given by the equation:

$$R_{total} = A\Delta n + B\Delta n^2 + C\Delta n^3. \tag{1.58}$$

The first term is the Shockley–Read–Hall recombination due to defects and traps, the second is the spontaneous emission due to radiative transition, and the third is the Auger recombination term. Auger recombination is non-radiative, occurs at high injection levels, and is a three-particle process. It becomes important in ternary and quaternary compounds of InP-based materials, and is evident in the long wavelength laser structures.

1.15.1 Spontaneous and stimulated emission

The radiative recombination process discussed above occurs spontaneously, and this is used in traditional LED structures. In lasers, stimulated emission is the source of light, and in this section the relationship between absorption, spontaneous emission and stimulated emission, first outlined by Einstein in 1917, is discussed. The derivations given here follow the approach outlined by Casey and Panish [4] and Agrawal [1].

It can be shown that the blackbody radiation law is given by

$$P(E) = \frac{8\pi \overline{n}^3 E^2}{h^3 c^3 (e^{E/kT} - 1)}, \tag{1.59}$$

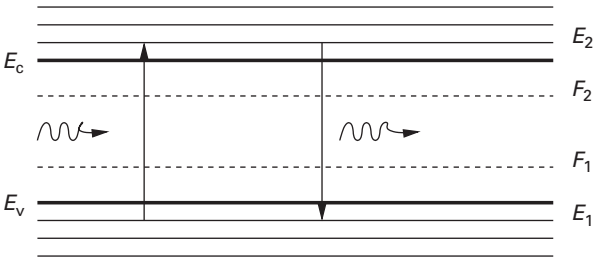

Fig. 1.24 Transitions from level E_1 to E_2 for absorption and from E_2 to E_1 for emission, F_1 and F_2 are the electron and hole quasi-Fermi levels respectively.

where $\overline{n}$ is the index of the material under consideration, h is Planck's constant, c is the speed of light in vacuum, E is the energy given by $h\nu$, ν is the frequency and k is Boltzmann's constant. This is the expression for the energy density blackbody radiation $P(E)$, and is in thermal equilibrium, when the input radiation is equal to the outgoing radiation.

For a semiconductor, consider the transitions from the conduction band to the valence band and also the reverse. The energy levels in each of these bands have to obey the Pauli exclusion principle, which implies only two carriers at each level. Thus, the band is a series of levels, as shown in Figure 1.24, and the transition energy for an electron from a level E_1 in the valence band to a level E_2 in the conduction band requires that an incident photon has energy given by $h\nu = E_2 - E_1$. Let the probability of this transition taking place be given by B_{12}, and let f_1 be the probability that an electron exists at level E_1 and $(1-f_2)$ be the probability that a vacancy occurs at level E_2. Also assume that the radiation density of photon energy incident on the semiconductor is given by $P(E_{21})$. Then the upward transition rate is given by

$$r_{12} = B_{12} f_1 (1 - f_2) P(E_{21}). \tag{1.60}$$

Note that f_1 and f_2 take the form of the Fermi–Dirac distribution

$$f_i = \frac{1}{e^{(E_i - F_i)/kT} + 1}, \tag{1.61}$$

where F_i is the corresponding quasi-Fermi level, k is Boltzmann's constant and T the temperature in Kelvin.

Similarly, the downward transition rate, now called the *stimulated transition*, is given as

$$r_{21}(\text{stim}) = B_{21} f_2 (1 - f_1) P(E_{21}), \tag{1.62}$$

where B_{21} is the transition probability, f_2 is the probability that an electron is present at E_2 and $(1 - f_1)$ is the probability that there is vacancy at E_1.

Finally, there is the spontaneous transition from E_2 to E_1, without any incident radiation involved, given by

$$r_{21}(\text{spon}) = A_{21} f_2 (1 - f_1). \tag{1.63}$$

In thermal equilibrium, the input radiation is equal to the output, the Fermi levels $F_1 = F_2$, and hence

$$r_{12} = r_{21}(\text{spon}) + r_{21}(\text{stim}). \tag{1.64}$$

Equating, simplifying and noting that $P(E_{21})$ is the blackbody radiation term,

$$P(E_{21}) = \frac{8\pi\overline{n}^3 E^2}{h^3c^3(e^{E_{21}/kT} - 1)} \tag{1.65}$$

$$= \frac{A_{21}f_2(1 - f_1)}{B_{12}f_1(1 - f_2) - B_{21}f_2(1 - f_1)} \tag{1.66}$$

$$= \frac{A_{21}}{B_{12}e^{E_{21}/kT} - B_{21}}. \tag{1.67}$$

Equating Equations (1.65) and (1.67) and separating them into temperature-dependent and temperature-independent terms give the following results:

$$A_{21} = \frac{8\pi\overline{n}^3 E^2}{h^3c^3}B_{21} \tag{1.68}$$

and

$$B_{21} = B_{12}. \tag{1.69}$$

These are Einstein's coefficients and their relationships with each other.

The condition under which stimulated emission dominates is an interesting one. This requires a non-equilibrium condition in which the presence of incident radiation is required. This results in the population densities in the conduction and valence bands to be different from the equilibrium condition. For stimulated emission to dominate, the stimulated emission rate, $r_{21}(\text{stim})$, needs to exceed the absorption rate r_{12}. Substituting from Equations (1.60) and (1.62),

$$B_{21}f_2(1 - f_1)P(E_{21}) > B_{12}f_1(1 - f_2)P(E_{21}). \tag{1.70}$$

Since $B_{21} = B_{12}$, this equation becomes

$$f_2(1 - f_1) > f_1(1 - f_2). \tag{1.71}$$

Substituting for f_1 and f_2 from Equation 1.61, this equation becomes

$$e^{(F_2 - F_1)/kT} > e^{(E_2 - E_1)/kT} \tag{1.72}$$

or

$$F_2 - F_1 > E_2 - E_1. \tag{1.73}$$

This implies that the difference in the quasi-Fermi levels is greater than the emission energy of the photon. If the emission is at bandgap energy, then the difference between quasi-Fermi levels needs to be greater than the bandgap energy E_g.

1.16 Carrier transport in semiconductors

Drift and diffusion are the two mechanisms whereby carriers are transported in semiconductors such that there is current flow. It will be assumed that thermal equilibrium will not be disturbed during these processes [2, 8, 10, 15].

1.16.1 Drift current

When an external electric field is applied to a semiconductor, it produces a force that will accelerate the electrons and holes in opposite directions as long as there are available energy states in the conduction and valence bands. The net drift of charge will produce a current which is the drift current. If the electric field is denoted as $\mathcal{E}$, the drift current densities for electrons and holes are written as

$$J_{\mathrm{n(drift)}} = qnv_{\mathrm{ndr}} = q\mu_{\mathrm{n}}n\mathcal{E} \tag{1.74}$$

$$J_{\mathrm{p(drift)}} = qpv_{\mathrm{pdr}} = q\mu_{\mathrm{p}}n\mathcal{E}, \tag{1.75}$$

where q is the charge on a particle (electron or hole), J is the surface density of current, v_{ndr} and v_{pdr} are the drift velocities of electrons and holes, respectively, and μ is the mobility.

1.16.2 Diffusion current

Electrons flow from a region of higher concentration to a region of lower concentration, producing a flux of electrons and an electron diffusion current which is in the opposite direction to the flux. The hole flow is such that the hole flux and the hole diffusion current are in the same direction since the holes are positively charged. The diffusion current densities for electrons and holes are given by

$$J_{\mathrm{ndiff}} = qD_{\mathrm{n}}\frac{dn}{dx} \tag{1.76}$$

$$J_{\mathrm{pdiff}} = -qD_{\mathrm{p}}\frac{dp}{dx}, \tag{1.77}$$

where D_{n} and D_{p} are the electron and hole diffusion coefficients respectively. The diffusion coefficient is related to the mobility μ by the Einstein relation:

$$D = \frac{\mu kT}{q}. \tag{1.78}$$

Hence,

$$\frac{D_{\mathrm{n}}}{\mu_{\mathrm{n}}} = \frac{D_{\mathrm{p}}}{\mu_{\mathrm{p}}} = \frac{kT}{q}. \tag{1.79}$$

Adding Equations (1.74)–(1.77),

$$J = (q\mu_{\mathrm{n}}n + q\mu_{\mathrm{p}}p)\mathcal{E} + qD_{\mathrm{n}}\frac{dn}{dx} - qD_{\mathrm{p}}\frac{dp}{dx}. \tag{1.80}$$

1.17 p–n junction

When a junction is formed by a p-type and an n-type semiconductor, holes move from the p to the n side across the metallurgical junction and electrons move in the opposite direction. There are concentration gradients of electrons and holes giving rise to diffusion. Furthermore, when the electrons leave the n region, positively ionised donor atoms remain behind and, similarly, negatively ionised acceptor atoms remain in the p region. These ionised donors and acceptors reside on both sides of the metallurgical junction and are not mobile. The length of this region increases as the diffusion continues. The resultant electric field is directed from the positive charge to the negative charge. This field builds up in such a way as to oppose the diffusion of the carriers in both directions across the junction. An equilibrium condition is reached and there is no net flow of current across the junction. The ionised region on both sides of the metallurgical junction is called the *depletion* or *space charge region*. The p–n junction is seen in Figure 1.25. The band diagram and space charge distribution of a p–n homojunction are shown in Figure 1.26. The general form of Poisson's equation for an abrupt junction where there is an abrupt change in the doping concentration is

$$\frac{d\mathcal{E}}{dx} = \frac{q}{\epsilon_s}(p - n + N_D - N_A), \tag{1.81}$$

where p is the hole concentration, n is the electron concentration and N_D and N_A are the ionised donor and acceptor concentrations respectively. If the metallurgical junction is the origin, the depletion region on the p side extends to $-x_p$ and on the n side to x_n. Poisson's equation is written for the depletion regions on either side of the metallurgical junction as

$$\frac{d\mathcal{E}}{dx} = -\frac{q}{\epsilon_s}N_A, \quad -x_p < x \leq 0 \tag{1.82}$$

$$\frac{d\mathcal{E}}{dx} = \frac{q}{\epsilon_s}N_D, \quad 0 < x \leq x_n, \tag{1.83}$$

where ϵ_s is the permittivity of the semiconductor material. The regions outside the depletion region are neutral regions and hence the electric field is zero. Equations (1.82) and (1.83) are solved using the boundary condition on the electric field to get

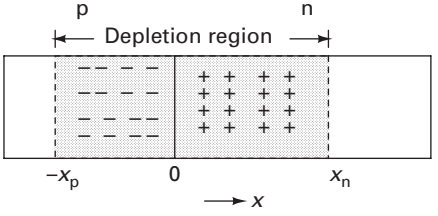

Fig. 1.25 p–n junction at equilibrium.

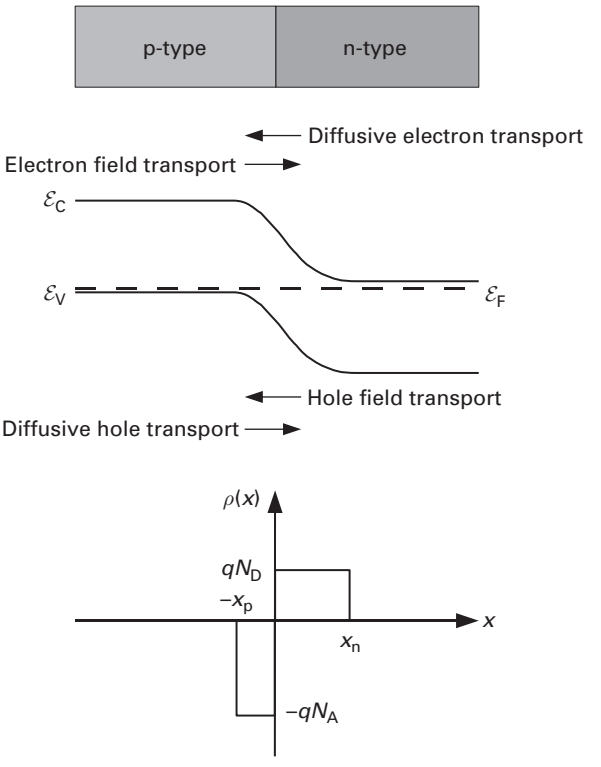

Fig. 1.26 p–n junction without externally applied voltage – band diagram (centre) and space charge distribution (bottom).

$$\mathcal{E} = -\frac{qN_A}{\epsilon_s}(x + x_p), \quad -x_p < x \leq 0 \tag{1.84}$$

$$\mathcal{E} = \frac{qN_D}{\epsilon_s}(x - x_n), \quad 0 < x \leq x_n. \tag{1.85}$$

The potential is related to the electric field by the equation

$$\mathcal{E} = -\frac{dV}{dx}. \tag{1.86}$$

Integrating Equations (1.84) and (1.85)

$$V(x) = \frac{qN_A}{2\epsilon_s}(x + x_p)^2, \quad -x_p < x \leq 0 \tag{1.87}$$

$$V(x) = -\frac{qN_D}{2\epsilon_s}(x - x_n)^2, \quad 0 < x \leq x_n. \tag{1.88}$$

1.17.1 The built-in potential

The built-in potential on the p side of the junction is the potential difference across the depletion region. It is determined similarly on the n side.

$$V_{\text{bip}} = \frac{qN_{\text{A}}}{2\epsilon_{\text{s}}}x_{\text{p}}^2 \tag{1.89}$$

$$V_{\text{bin}} = \frac{qN_{\text{D}}}{2\epsilon_{\text{s}}}x_{\text{n}}^2. \tag{1.90}$$

The total built-in potential across the junction is

$$V_{\text{bi}} = (V_{\text{bip}} + V_{\text{bin}}) \tag{1.91}$$

$$= \frac{q}{2\epsilon_{\text{s}}}[N_{\text{A}}x_{\text{p}}^2 + N_{\text{D}}x_{\text{n}}^2]. \tag{1.92}$$

The continuity of the electric field across the junction at $x = 0$ requires that

$$N_{\text{A}}x_{\text{p}} = N_{\text{D}}x_{\text{n}}. \tag{1.93}$$

It is assumed that the dopants are fully ionised and the total ionised positive charge per unit area on the n side is equal to the total ionised negative charge per unit area on the p side. At thermal equilibrium, there is no net current flow and hence the drift and diffusion currents are equal. The electron current is

$$J_{\text{n}} = 0 \tag{1.94}$$

$$= J_{\text{ndrift}} + J_{\text{ndiff}} \tag{1.95}$$

$$= q\mu_{\text{n}}n\mathcal{E} + qD_{\text{n}}\frac{dn}{dx}. \tag{1.96}$$

The hole current is written as

$$J_{\text{p}} = 0 \tag{1.97}$$

$$= J_{\text{pdrift}} + J_{\text{pdiff}} \tag{1.98}$$

$$= q\mu_{\text{p}}p\mathcal{E} - qD_{\text{p}}\frac{dp}{dx}. \tag{1.99}$$

When the net hole current is zero, and with the electric field equal to the gradient of the potential, it may be shown that

$$V_{\text{bi}} = \frac{kT}{q}\ln\frac{N_{\text{A}}N_{\text{D}}}{n_{\text{i}}^2}. \tag{1.100}$$

It has been assumed that there is full ionisation of the dopant impurity levels such that the majority carrier concentrations are the doping concentrations and the equilibrium concentrations are related by

$$n_0p_0 = n_{\text{i}}^2. \tag{1.101}$$

1.17.2 The depletion layer width

The widths of the depletion layer in the p- and n-type semiconductors may be calculated. The maximum electric field occurs at the metallurgical junction, $x = 0$. This is given by

$$\epsilon_{\text{s}}\mathcal{E}_{\text{max}} = qN_{\text{D}}x_{\text{n}} = qN_{\text{A}}x_{\text{p}}. \tag{1.102}$$

Using the Equations (1.92) and (1.93) with

$$| V_{bi} | = \frac{\mathcal{E}_{max}}{2}[x_n + x_p] \tag{1.103}$$

$$W = x_n + x_p \tag{1.104}$$

$$= \sqrt{\frac{2\epsilon_s}{q}\left(\frac{1}{N_D} + \frac{1}{N_A}\right) | V_{bi} |}. \tag{1.105}$$

1.17.3 The depletion capacitance

The depletion capacitance is the capacitance at the p–n junction. The depletion layer is modelled as a parallel plate capacitor. The capacitance is written as

$$C_j = \frac{\epsilon_s A}{W}, \tag{1.106}$$

where A is the area of the p–n junction and W is the depletion layer width given by Equation (1.105). The junction capacitance is given by

$$C = A\sqrt{\frac{q\epsilon_s N_A N_D}{2V_{bi}(N_A + N_D)}}. \tag{1.107}$$

1.17.4 p–n junction under bias

At thermal equilibrium, the total electrostatic potential across the p–n junction is the built-in potential, V_{bi}, and the potential difference between the p and n regions is qV_{bi}. If now a voltage V_A is applied with the positive terminal connected to the p side and the negative to the n side, the junction is forward-biased and the total electrostatic potential across the junction is $V_{bi} - V_A$, resulting in a reduction of the depletion layer width. A potential barrier was formed at thermal equilibrium restricting the motion of the majority carriers. The application of the forward bias reduces the height of the barrier. If, on the other hand, a voltage is applied with the positive terminal connected to the n side and the negative terminal to the p side, the electrostatic potential across the junction is $V_{bi} - (-V_A)$ and the height of the barrier is increased with the reverse bias. The depletion widths and the energy band diagrams are shown in the figure. The width of the depletion layer is given by

$$W = \sqrt{\frac{2\epsilon_s}{q}\left(\frac{N_D + N_A}{N_A N_D}\right)(V_{bi} \mp V_A)}. \tag{1.108}$$

1.17.5 Current–voltage characteristics

The total current density in a p–n junction is given as:

$$J = q\left[\frac{D_n n_{p0}}{L_n} + \frac{D_p p_{n0}}{L_p}\right]\left[\exp\left(\frac{qV_A}{kT}\right) - 1\right], \tag{1.109}$$

where

$$L_n = \sqrt{D_n \tau_n} \tag{1.110}$$

$$L_p = \sqrt{D_p \tau_p} \tag{1.111}$$

$$n_{p0} = \frac{n_i^2}{N_A} \tag{1.112}$$

$$p_{n0} = \frac{n_i^2}{N_D}. \tag{1.113}$$

The current density expression now reduces to

$$J = J_0 \left[\exp\left(\frac{qV_A}{kT} \right) - 1 \right] \tag{1.114}$$

where

$$J_0 = q n_i^2 \left[\sqrt{\frac{D_n}{\tau_n}} \frac{1}{N_A} + \sqrt{\frac{D_p}{\tau_p}} \frac{1}{N_D} \right], \tag{1.115}$$

where D_n and D_p are the Einstein coefficients for electrons and holes and τ_n and τ_p are the electron and hole lifetimes.

1.18 Schottky diode

Another important type of semiconductor junction is the *Schottky diode*, a metal–semiconductor junction.

Its band diagram is shown in Figure 1.27, assuming that the semiconductor layer is n-doped, that the doping concentration is constant throughout the layer (homogeneous doping), and that the Boltzmann approximation for the Fermi distribution is

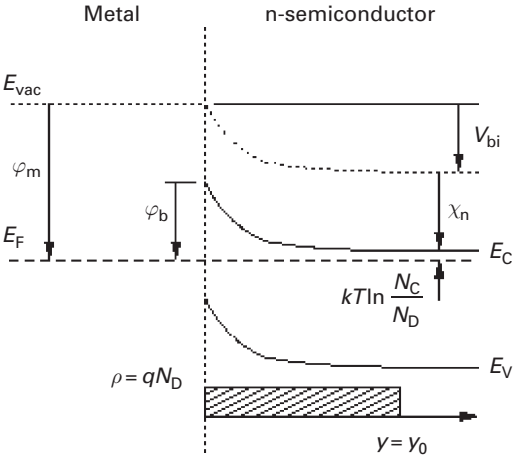

Fig. 1.27 Band diagram of a Schottky contact on a homogeneously n-doped semiconductor layer, without an externally applied voltage. The bottom graph shows schematically the extension of the space charge region.

valid. We see that under ideal circumstances, the Schottky barrier height φ_b is the difference between the metal work function φ_m and the electron affinity χ_n. In practice, however, the effective Schottky barrier height φ_b is also influenced by states at the metal–semiconductor interface and shows only a small dependence on the metal work function. On GaAs, $\varphi_b \approx 0.8\,\text{eV}$.

The built-in voltage can be easily calculated:

$$V_{bi} = \varphi_b - kT \ln \frac{N_C}{N_D}, \tag{1.116}$$

where N_C is the density of states in the conduction band and N_D the semiconductor doping concentration.

The Schottky barrier φ_b causes a depletion of the semiconductor layer immediately adjacent to the metal–semiconductor interface. Devoid of electrons, the positively charged ionised donors remain and form a *space charge region* with a space charge density $\rho = qN_D$. It is indicated in the bottom graph of Figure 1.27 – we make the usual 'box shape' assumption for the space charge region, i.e. we assume the space charge concentration to be constant throughout until $y = y_0$, then ending abruptly.

For a homogeneously doped semiconductor with a permittivity of ϵ_s and a doping concentration of N_D,

$$y_0 = \sqrt{\frac{2\epsilon_s V_{bi}}{qN_D}} \tag{1.117}$$

without any externally applied voltage.

1.19 Heterostructures

The ability to mix semiconductors of different chemical composition in a single crystal gives an important degree of freedom in device design. The combination of semiconductor materials of different stoichiometry in a single crystal is called a *heterostructure*.

Of foremost interest is the ability to change the energetic width of the forbidden gap – the bandgap energy, or band gap in short. This is shown in Figure 1.28 for some popular atomic and binary semiconductor materials. We note that changing the stoichiometry not only modifies the bandgap energy, but also the lattice constant, which can be understood as an average distance between the atoms in the crystal. This change in lattice constant is a major complication when designing devices, but we will exclude it for now by considering the material system (Al,Ga)As, where the lattice constant is almost independent of stoichiometry.

The ability to change bandgap through stoichiometry opens up several interesting design options.

- We may, for example, introduce a built-in electric field for one carrier species, but not for the other – schematically shown in Figure 1.29. This is a p-type semiconductor which has a smaller bandgap on the left-hand side ($E_{g,I}$) than on the right-hand side.

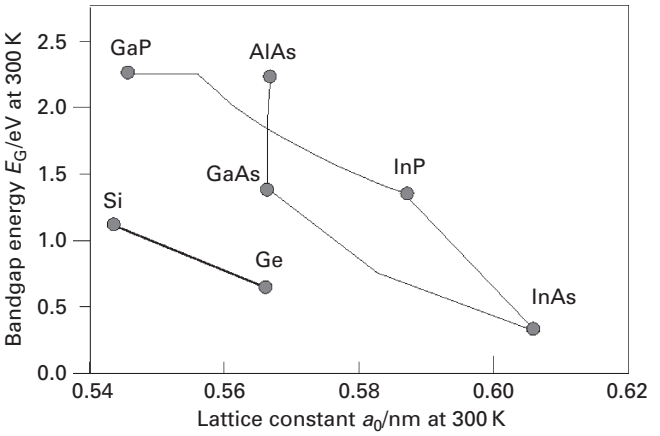

Fig. 1.28 Bandgap energy and lattice constant for several popular semiconductor materials.

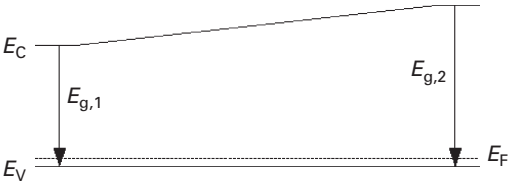

Fig. 1.29 Hypothetical band diagram of a p-doped graded heterostructure.

This could be done by starting with GaAs and gradually increasing the aluminium content while progressing to the right. Due to the p-type doping, the valence band stays approximately equidistant to the Fermi energy E_F (neglecting the change in the valence band density of states N_V), which is constant in thermodynamic equilibrium.[1] Due to the change in bandgap energy, the conduction band energy will change strongly and provide a built-in drift field for electrons, which in this schematic will be accelerated from right to left.

We will later use such a structure to accelerate the electrons in the base of a heterostructure bipolar transistor.

- Or we may abruptly change the bandgap by an abrupt modification of the stoichiometry (see Figure 1.30). In this case, we use an n-type semiconductor material, so the conduction bands remain approximately lined up horizontal (save for the stoichiometry-induced change in the conduction band density of states), but the change in bandgap results in a significant additional energy barrier for holes, which will keep them from moving from region 1 into region 2. This *carrier confinement* is at the heart of any semiconductor laser structure, and will also be used in heterostructure bipolar transistors. Note that a comparable energy barrier does not exist for electrons – an energy barrier has been created for one carrier species only, a feat possible only through the introduction of semiconductor heterostructures.

[1] The picture is a simplification because changing the stoichiometry also changes the density of states in the valence band, so there will be some variation in the E_F to E_V distance, which has been omitted.

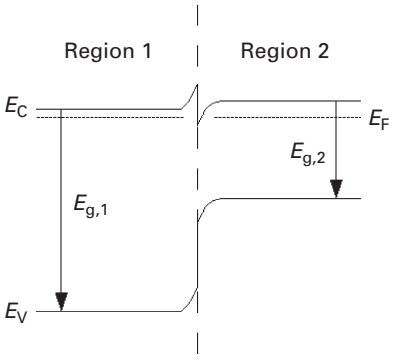

Fig. 1.30 Energy band diagram of an abrupt transition between two materials in a semiconductor heterostructure.

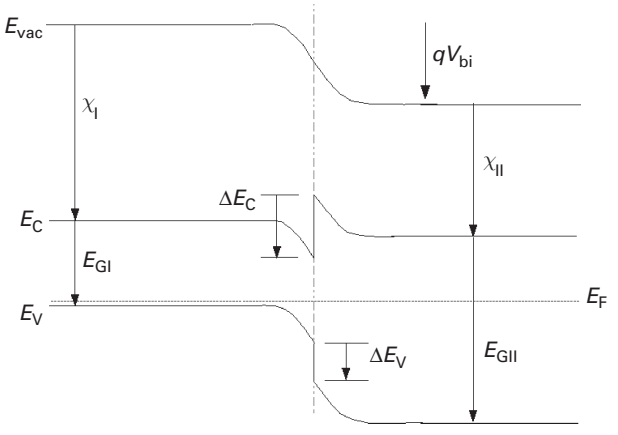

Fig. 1.31 Constructing heterostructure band diagrams using Anderson's rule.

1.19.1 Constructing heterostructure band diagrams

To efficiently use heterostructure band diagrams in the understanding of high-speed electronic and optoelectronic devices, we have to be able to construct their band diagrams. A simple procedure shall be described here.

It uses a modification of *Anderson's rule*, which has been a proven technique to draw the band diagram of the important SiO_2–Si interface. Anderson's rule postulates that the vacuum energy level is continuous and uses the electron affinities, i.e. the energetic spacing between the vacuum level and the conduction band, to calculate the band alignment in an abrupt heterostructure. The electron affinity χ is material-dependent.

When constructing the band diagrams, see Figure 1.31; we start out with the Fermi energy E_F, which in thermodynamic equilibrium is constant throughout the structure. We next draw conduction and valence bands *far away from the interface* between the two materials, which requires knowledge of the doping type and concentration, the bandgap energy and the densities of state as described in the introductory review section.

Next, we use knowledge of the electron affinities χ in the two materials to draw the vacuum level, again far away from the interface. Poisson's equation can be used to calculate the exact potential in the interfacial region, which is used to draw the continuous vacuum energy level. The material properties remain constant right up to the interface, so we can draw the conduction and valence bands to be perfectly parallel to the vacuum level.

The resulting conduction and valence bands show *discontinuities* at the interface between the two materials, in direct consequence of the the different electron affinities and the continuity of the vacuum energy level.

The built-in potential V_{bi} can be calculated as follows (refer again to Figure 1.31). We assume here for simplicity's sake that the Boltzmann equation can be used in lieu of the Fermi–Dirac function:

$$q \cdot V_{\mathrm{bi}} = \chi_{\mathrm{I}} - \chi_{\mathrm{II}} + E_{\mathrm{G,I}} + kT \cdot \ln\left(\frac{N_{\mathrm{V,I}} N_{\mathrm{C,II}}}{N_{\mathrm{A,I}} N_{\mathrm{D,II}}}\right). \tag{1.118}$$

Assume that you externally apply a voltage $-V_{\mathrm{bi}}$ to the structure, which compensates the built-in potential – the energy bands would then be constant within the two regions of the heterostructure (flatband condition); now you easily recognise that

$$\Delta E_{\mathrm{C}} = \chi_{\mathrm{I}} - \chi_{\mathrm{II}} \tag{1.119}$$

and

$$\Delta E_{\mathrm{V}} = E_{\mathrm{G,I}} - E_{\mathrm{G,II}} - \Delta E_{\mathrm{C}} = \Delta E_{\mathrm{G}} - \Delta E_{\mathrm{C}}. \tag{1.120}$$

However, in reality, the experimentally determined band discontinuities of heterostructures do not agree well with the values predicted using the electron affinities. This has to do with the different interface conditions between a free surface (used to determine the electron affinities) and a semiconductor heterostructure.

Anderson's rule can still be used, however. Note that only the difference of the electron affinities matters, not their absolute values. Hence, you can place the vacuum level at an arbitrary distance from the conduction band when drawing the band diagram, provided that the difference in the hypothetical electron affinities agrees with the *experimentally determined* ΔE_{C}.

1.19.2 Band line-up

Abrupt heterostructures can have three fundamental band alignments – refer to Figure 1.32 for a schematic representation:

(i) In a *type 1* heterojunction, the conduction band of the material with the lower bandgap is below the conduction band of the material with the higher bandgap, but the valence band of the lower-bandgap material is above the valence band of the higher-bandgap material. The smaller bandgap is hence fully within the larger bandgap.

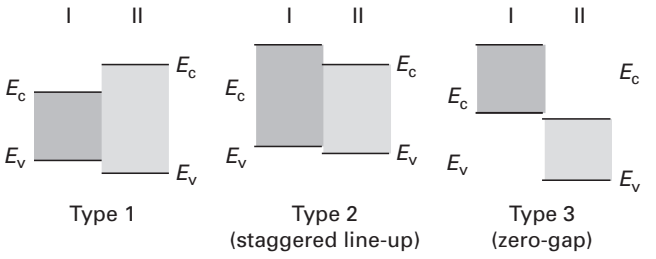

Fig. 1.32 Schematic representation of heterostructure line-ups.

(ii) In a *type 2* heterojunction, the conduction band and the valence band of one material are below their counterparts in the other material. This is sometimes also referred to as a *staggered line-up*.

(iii) Finally, in a *type 3* heterojunction, the valence band in one material is above the conduction band in the other. This is called a *zero-gap* configuration.

In current practical devices, the type 1 line-up is by far the most common.

1.19.3 Lattice mismatch

As already observed in Figure 1.28, changing the stoichiometry will generally also modify the lattice constant. When combining materials with different lattice constants, the mismatch will create strong mechanical strain at the interface (experienced as tensile strain by the material with the smaller lattice constant and as compressive strain by other materials).

Please refer to Figure 1.33. We shall visualise in a schematic fashion the problem of lattice mismatch, taking the important Si/SiGe heterostructure as an example.

In this example, a thin SiGe layer shall be sandwiched between two thick Si layers.[2] Provided that the thickness of the SiGe layer remains below a certain *critical thickness*, all of the lattice mismatch can be compensated for by *elastically* straining the thin layer (and a small fraction of the neighbouring layers). This case is also called the *pseudomorphic* case, a term which we will encounter later on, e.g. in the discussion of modern field effect transistor (FET) structures.

If, however, the strained layer thickness is significantly increased beyond the critical thickness, the mechanical forces at the interface become so large that they are able to break crystalline bonds – a crystal defect is created which will have detrimental effects in both optoelectronic and electronic structures and is hence to be avoided (but for a very few special cases, where this *plastic* strain relaxation is used deliberately in areas of the device devoid of mobile charge carriers).

Hence, the critical thickness is a parameter which must be carefully obeyed in heterostructure device design. It depends on both the lattice mismatch and the elements forming the heterostructure.

[2] 'Thin' here means that the whole layer can be deformed by the mismatch-generated strain, while 'thick' means that the largest part of the layer remains unstrained.

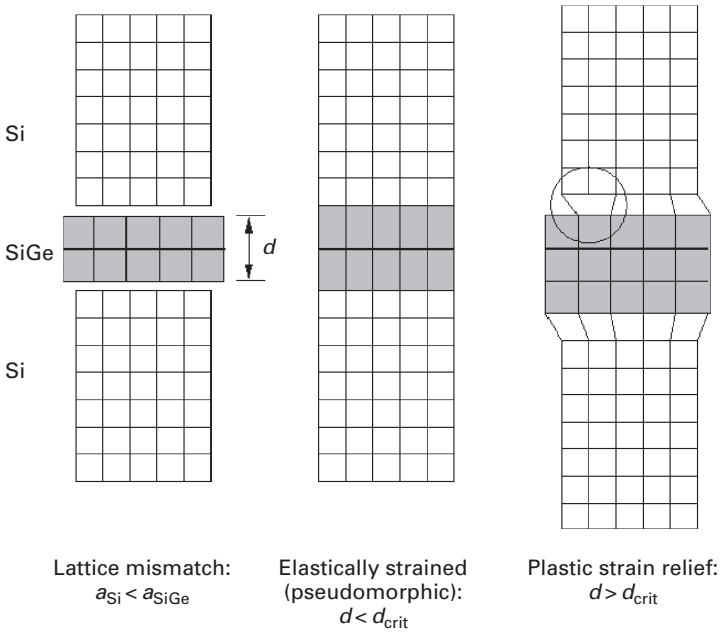

Fig. 1.33 Schematic representation of lattice mismatch in heterostructures.

This introductory section on heterostructures concludes with what 2000 Nobel laureate Herbert Kroemer has called the *Central Design Principle* of semiconductor heterostructures:

> Heterostructures use energy gap variations in addition to electric fields as forces acting on holes and electrons to control their distribution and flow [7].

Our future treatment of high-speed electronic and optoelectronic devices will only exemplify this fundamental observation.

1.20 Silicon–germanium heterostructures

Until the late 1980s, practical electronic and optoelectronic devices, if they included compound semiconductor materials, were dominated by materials combining elements from the third and fourth columns of the periodic table of elements, such as GaAs or InP. However, compound semiconductors may also be formed from elements in the fourth column – elements which already are semiconductors. One example is SiC, which has been investigated extensively as a blue-light emitter. As an aside, SiC under its old trademark of 'carborundum' was the first semiconductor material for which light emission was ever observed and is finding renewed interest for high-power transistors [11].

The currently most important group IV–IV semiconductor material, however, is the silicon–germanium alloy which shall receive special treatment here commensurate with its importance.

Table 1.5 Basic properties of silicon and germanium

Property	Silicon	Germanium	Unit
Lattice type	Diamond	Diamond	
Lattice constant	0.5431	0.5657	nm
Direct band gap	3.40	0.80	eV
Indirect band gap	1.11	0.664	eV
Indirect bandgap direction	{100}	{111}	
Relative dielectric constant	11.9	16.2	

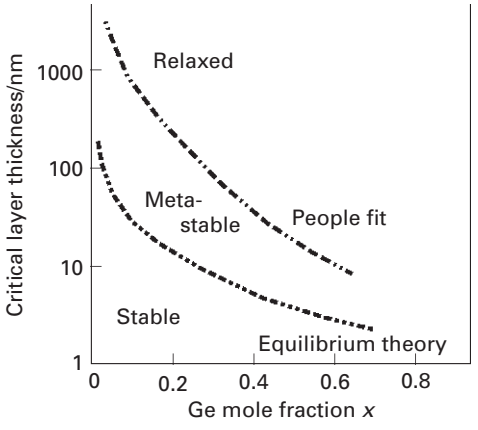

Fig. 1.34 Critical thickness of a strained SiGe layer on Si.

Table 1.5 [13] summarises some fundamental properties of silicon and germanium. As we see, both are indirect semiconductors. Of special interest is the difference in band gap, which will allow to build efficient heterostructure devices. However, the significant difference of the relative dielectric constant (and consequently the refractive index) has also been used in photonic waveguiding devices.

We also note that the lattice constant is quite different – the ratio of lattice constants is

$$\frac{a_{\mathrm{Ge}}}{a_{\mathrm{Si}}} = 1.042$$

for a mismatch of 4.2%.

Therefore, any SiGe heterostructure will be strained, and the strain has significant consequences. In most cases, a pseudomorphic heterostructure free from crystal defects will be desired, and hence the critical layer thickness has to be obeyed.

There is, however, already some discussion about the value of the critical layer thickness. Refer to Figure 1.34 adapted from [5], which plots the critical thickness of a strained $Si_{1-x}Ge_x$ layer on relaxed silicon. This is the case found in Si/SiGe heterostructure bipolar transistors (HBTs), where the base is formed from a SiGe alloy, while the emitter and collector layers are silicon.

There are two substantially different curves for the critical thickness as a function of the germanium mole fraction x.

(i) The equilibrium theory limit constitutes a safe upper limit in that strained layers grown with combinations of Ge content and thickness will remain stable even under high-temperature processing.
(ii) The *People fit* [9] takes experimental data into account. Here, depending on the growth temperature, much higher products of layer thickness and Ge mole fraction will still result in defect-free layers, provided that they do not encounter high-temperature processing after layer deposition.

The region between the equilibrium-theory and People-fit curves is called the *metastable region*. Many practical SiGe devices possess Ge fraction and layer thickness combinations in this region.

The strain also very substantially affects the band structure of SiGe heterojunctions. This is important to understand the concepts of SiGe heterostructure devices further down. In the above example of an elastically strained SiGe layer on a relaxed silicon layer, the heterojunction forms a type 1 interface, i.e. the SiGe band gap is located energetically in the forbidden gap of silicon. Most of the bandgap difference is reflected in the valence band discontinuity on an abrupt heterostructure. If, however, we place a thin strained Si layer on a relaxed SiGe layer, the heterojunction will be of type 2, the staggered line-up configuration, with the Si conduction band below the SiGe conduction band. The resulting conduction band discontinuity will further down be used to construct n-channel Si/SiGe heterostructure field effect transistors (HFETs).

The effect of layer composition has been compiled by Schäffler [12] into a convenient chart, shown in Figure 1.35.

Its use shall be demonstrated using the following example. Suppose you are looking for the band alignment of a strained $Si_{0.1}\,Ge_{0.9}$ layer on relaxed $Si_{0.4}\,Ge_{0.6}$. In this case, $x_{relaxed} = 0.9$ and $x_{strained} = 0.6$. In this case, we read $\Delta E_C = 0$ and $\Delta E_V = +220$ meV.

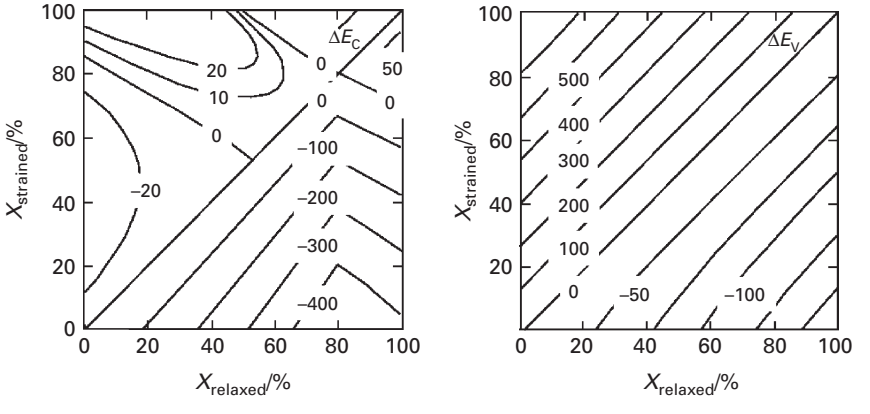

Fig. 1.35 Conduction band (ΔE_C) and valence band (ΔE_V) discontinuities of $Si_{1-x}Ge_x$ heterostructures, depending on the relaxed-layer and strained-layer Ge mole fraction x. The discontinuity values are listed in meV. Graphs adopted from Schäffler (1995), Ref. 12.

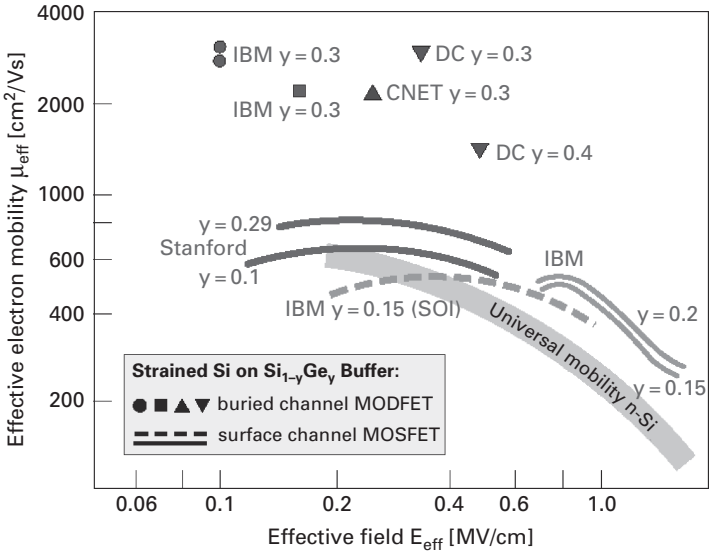

Fig. 1.36 Electron mobility enhancement in strained-Si MOSFET channels [6]. Used with permission from Oerlikon Systems.

Another interesting effect of strain in Si/SiGe heterostructures is that it modifies mobility, an effect investigated for performance enhancement in Si MOSFETs. Here, a thin silicon layer is deposited on top of a relaxed SiGe buffer. The SiGe buffer does not carry any current, but provides a means of introducing a tensile lateral strain into the silicon channel layer above. Depending on the electric field in the channel, a mobility enhancement of 30% or more may result, compared to the Si universal mobility curve (see Figure 1.36). [6]

1.21 Problems

(1) Consider a three-dimensional potential well which is infinite such that the following conditions are satisfied:

$$V(x, y, z) = 0, -a < x < a, -a < y < a, -a < z < a, \tag{1.121}$$

Outside the well

$$V(x, y, z) = \infty. \tag{1.122}$$

Show that the energy is quantised and determine its form.

(2) (a) Determine the amplitudes of the transmitted and reflected waves in the finite potential barrier. Use these results to determine the transmission and reflection coefficients and hence the tunnelling probability (also called the *transmissivity*) given in Equation (1.25).

(b) A potential barrier has width $a = 30$ Å and height $V_0 = 0.5$ eV. An electron is incident on this barrier. Sketch the transmissivity function.

(c) The barrier width is reduced to 5 Å. Sketch the transmissivity function. Comment on the difference as the barrier width is reduced.

(3) For the Kronig–Penney model, obtain the solution of the transcendental equation and show the allowed energy bands (MATLAB is useful in this problem).

(4) A sample of GaAs is doped with a background concentration of $N_A = 3 \times 10^{15}\,cm^{-3}$ acceptors. Then, $10^{19}\,cm^{-3}$ donors are added. Find the room temperature concentrations of electrons and holes in the original material and the material that results after the addition of the donors. Draw the band diagram for each of the materials.

(5) A silicon ingot is doped with $10^{17}\,cm^{-3}$ arsenic atoms. Find the carrier concentrations and the Fermi level at 300° K. Assume complete ionisation of impurity atoms. Draw the band diagram. Show the Fermi level and use the intrinsic Fermi level as the energy reference. Repeat for a temperature of 77° K.

(6) (a) The energy band gap for GaAs at 300 K is 1.42 eV. Assume that the Fermi energy level is at mid-band. Calculate the probability that an energy state at $E = E_c + kT/2$ is occupied by an electron.
(b) What is the probability that the energy state at $E = E_v - kT/2$ is empty?
(c) Using the density of states function $g(E)$, determine the volume density of states between 0 and 2 eV. (Integrate $g(e)dE$.)

(7) A sample of InP is doped with 5×10^{16} tellurium atoms/cm^3 and $2 \times 10^{15}\,cm^{-3}$ zinc atoms. Calculate the electron and hole concentrations.

(8) A sample of GaAs is illuminated with light of intensity 1.5 mW cm^{-2} at a wavelength of $\lambda = 470$ nm. The area of the illuminated surface is 15 mm^2. If the carrier lifetimes are 10 ns, how many photons are incident on the surface of the GaAs sample? If there is uniform absorption of the photons within 1 μm of the sample surface, determine the equilibrium concentrations of electrons and holes in the dark and the excess carrier concentrations when the sample is illuminated.

(9) (a) An n^+–p diode has a long p region. The current I is measured at a constant forward bias of 500 mV. Derive an expression for the fractional change in current $\Delta I/I$ resulting from a temperature change of ΔT. Evaluate this expression at $T = 300$ K. Assume that the diode current is dominated by recombination of electrons in the neutral p region and consider the temperature dependence to be due solely to the factors that have an exponential dependence on temperature.
(b) Suppose that part of the diode current results from recombination in the depletion region. How will this affect the sensitivity of the temperature measurement?

(10) A Silicon p–n junction has $5 \times 10^{17}\,cm^{-3}$ donor atoms and $4 \times 10^{19}\,cm^{-3}$ acceptor atoms. The junction area is 150 μm^2. Determine the junction capacitance given that the reverse bias is 5 V. How does this change for the same forward bias?

(11) It is found experimentally that a Schottky barrier is formed when Al is evaporated on n-type GaAs with a donor concentration of $4 \times 10^{15}\,cm^{-3}$. Al has a work function of 4.36 V and GaAs has an electron affinity of 4.07 V.
(a) Determine the built-in voltage V_{bi}, the depletion layer width W and the capacitance at zero bias, assuming no surface states.

(b) If the Fermi level at the surface is pinned so that

$$q\phi_0 = \frac{1}{3}E_g$$
$$q\phi_B = (E_g - q\phi_0),$$

determine the same quantities as in part (a) with a reverse bias of 1 V.

(12) An n^+-GaAs/p-AlGaAs heterojunction is formed with $N_D = 10^{19}\,cm^{-3}$ and $N_A = 5 \times 10^{17}\,cm^{-3}$. Draw the band diagram and determine the following quantities:
(a) The electric field $\mathcal{E}(x)$ and the potential difference $V(x)$ at the junction.
(b) The built-in potentials on either side of the junction and the total built-in potential, V_{bi}.
(c) The depletion widths in the two regions.
(d) If a forward bias of 3 V is applied, calculate the depletion widths.
(e) Calculate the capacitance of this diode.
(f) Calculate the current in the diode.

References

[1] Agrawal G. P., Dutta N. K. (1993). *Semiconductor Lasers*, Van Nostrand Reinhold.
[2] Anderson B. L., Anderson R. L. (2005). *Fundamentals of Semiconductor Devices*. McGraw-Hill.
[3] Bhattacharya P. (1997). *Semiconductor Optoelectronic Devices*, 2nd edn. Prentice Hall.
[4] Casey H. C., Panish M. B. (1978). *Heterostructure Lasers Part A: Fundamental Principles*. Quantum electronics – principles and applications, Academic Press.
[5] Gruhle A. (1994). *SiGe Heterojunction Bipolar Transistors of Silicon-based Millimeter Wave Devices*. Springer Verlag, 149–189.
[6] Hackbarth T., Zeuner M., König U. (2002). The future of SiGe beyond HBT applications. *Uniaxis chip Magazine*, July 10–12.
[7] Kroemer H. (1982). Heterostructure bipolar transistors and integrated circuits. *Proceedings of the IEEE 70*. 1 (January), 13–25.
[8] Neaman D. A. (2003). *Semiconductor Physics and Devices: Basic Principles*. McGraw-Hill.
[9] People R., Bean J. C. (1985). Calculation of critical layer thickness versus lattice mismatch for Ge_xSi_{1-x}/Si strained-layer heterostructures. *Appl. Phys. Lett. 47*, 322–324.
[10] Pierret R. F. (2003). *Advanced Semiconductor Fundamentals*. Modular Series on Solid State Devices, Vol. VI. Prentice Hall.
[11] Round H. J. (1907). A note on Carborundum. *Elect.World 49,* 10, 309.
[12] Schäffler F. (1995). *Properties of Strained and Relaxed Silicon Germanium* of EMIS Data Reviews. 12. IEE INSPEC, 10–12.
[13] Schäffler F. (1997). High mobility Si and Ge structures. *Semicond. Sci. Technol. 12,* 10, 1515–1549.
[14] Singh J. (1994). *Semiconductor Devices – An Introduction*. McGraw-Hill.
[15] Streetman B., Banerjee S. (2000). *Solid State Elecronic Devices*, 5th edn. Prentice Hall.